Journal of Applied Polymer Science

Poly(lactic acid)–layered silicate nanocomposites: The effects of modifier and compatibilizer on the morphology and mechanical properties

Eda Acik Cumkur,[1] Touffik Baouz,[2] Ulku Yilmazer[1]

[1]Department of Chemical Engineering, Middle East Technical University, Ankara 06800, Turkey

[2]Laboratoire des Matériaux Organiques (LMO), Département de Génie des Procédés, Faculté de Technologie, Université de Bejaia, Bejaia 06000, Algeria

Correspondence to: U. Yilmazer (E-mail: yilmazer@metu.edu.tr)

ABSTRACT: Poly(lactic acid) (PLA) based nanocomposites were prepared to investigate the effects of types of nanoclays. Five different organically modified nanoclays (Cloisites®15A, 25A, and 30B, and Nanofils®5 and 8) were used. Two rubbery compatibilizers, ethylene-glycidyl methacrylate (E-GMA) and ethylene-butyl acrylate-maleic anhydride, were used in the nanocomposites as compatibilizer-impact modifier. The degree of clay dispersion, the chemical compatibility between the polymer matrix and the compatibilizers, and changes in the morphology and mechanical properties of the nanocomposites were investigated. The mechanical properties and the morphological studies showed that the interactions between the different compatibilizers and PLA resulted in different structures and properties; such that the dispersion of clay, droplet size of the compatibilizer, and tensile properties were distinctly dependent on the type of the compatibilizer. Compatibility between C25A, C30B, and E-GMA resulted in the best level of dispersion, leading to the highest tensile modulus and toughness among the compositions studied. In the mentioned nanocomposites, a network structure was formed owing to the high reactivity of the epoxide group of GMA towards the PLA end groups resulting in high impact toughness. © 2015 Wiley Periodicals, Inc. J. Appl. Polym. Sci. **2015**, *132*, 42553.

KEYWORDS: Poly(lactic acid); organically modified nanoclay; nanocomposite

Received 19 April 2015; accepted 27 May 2015

DOI: 10.1002/app.42553

INTRODUCTION

Poly(lactic acid) (PLA) is a biodegradable, linear, aliphatic polyester. Decreased production cost of this polymer along with the recent advances in polymerization technologies makes it to be economically competitive compared with the petroleum based commercial polymers. Thus, PLA becomes attractive for several industrial applications such as packaging, textile, and automotive industries.[1–3] Even though PLA has numerous advantages such as being eco-friendly, having comparable cost with petroleum based polymers, and having high strength and modulus, its intrinsic brittleness restricts its utilization in pristine form.

Similar to the conventional plastics, blending PLA with flexible polymers or making composites using inorganic or natural fillers are the potential methods to improve the mechanical properties of PLA. Blends of brittle polymers such as PLA and polystyrene (PS) with flexible polymers usually show toughening; however, this enhancement comes together with reductions in tensile strength and tensile modulus. Reinforcement of biodegradable polymers through the addition of macro or nano-scale reinforcements can be a useful method in production of eco-friendly nanocomposites for various applications.[4] Even though incorporation of these rigid fillers results in improvement in modulus, it usually causes reductions in elongation at break.

The key parameter in obtaining reinforced material properties by blending or adding fillers is the interactions between the constituents. The interface between the materials forming the composite structure might involve multiple bonding types such as mechanical, chemical, and/or physical bonding. Presence of either of these interactions depends upon the structure of the additive used with the matrix polymer. There are some studies concerning the structure of the clay modifier in the literature. Varying the hydrophobicity of the organic modifier was shown to be one of the dominating parameters in formation of the nanocomposite structure, that controls the degree of diffusion of polymer chains into the layers of the clay.[5] Not only the characterization studies but also computationally determined solubility parameters showed that among the three types of clay (Cloisites 15A, 25A, and 30B), Cloisite 30B (C30B) is the most

suitable organoclay exhibiting good dispersion and exfoliation in PLA matrix. This was explained with the enthalpic interactions between the diols in the modifier of C30B and the carbonyl moieties of PLA. It was also indicated that as the degree of interaction and dispersion increased, crystallinity of the nanocomposites decreased due to decreased chain mobility. Mechanical properties were also affected by the interactions between the matrix and the filler. Storage modulus increased compared to that of pristine polymer when effective dispersion of the filler was achieved. C30B was also shown to have the highest affinity to the polyethylene glycol (PEG) plasticizer among the three alternatives (Cloisites 20A, 25A, and 30B).[6] The interactions between PLA and C30B modifier were explained by hydrogen bonding between the carbonyl group in the main chain of PLA molecules and the hydroxyl group in the modifier.

Toughening PLA by blending it with elastomeric polymers depends also on interfacial interactions between the components. Several different polymers were blended with PLA, such as linear low density polyethylene (LLDPE),[7] polycaprolactone (PLC),[8–10] poly(butylene succinate) (PBS),[11] and polyurethane (PU).[12] A comprehensive review on toughening of PLA was made by Anderson *et al.*[13] To have enhanced interactions between the materials and fine dispersion of the impact modifier, chemically complementary groups are preferred in the rubber structure for reactive blending. For instance, epoxide group is reactive towards the functional end groups of PLA (hydroxyl and carboxyl groups). This leads to the utilization of glycidyl methacrylate (GMA) copolymers in PLA blends. Oyama[14] studied toughening of PLA via melt blending with poly (ethylene-*co*-glycidyl methacrylate) (E-GMA). The blends of low molecular weight PLA with 20 wt % E-GMA showed almost 200% elongation at break compared to 5% elongation at break in pristine PLA. Notched Charpy impact strength of this blend was also two times that of neat PLA. Annealing of injection molded specimens at a temperature above the glass transition of PLA (90°C) resulted in 50-fold increase in the impact toughness of the blend. Styrene-butadiene-styrene block copolymer (SEBS) was also used to toughen PLA together with E-GMA.[15] Notched Izod impact strength of 92 kJ/m^2, which is almost 30% higher than the previous study mentioned, and an elongation at break of 185% were achieved with PLA/SEBS/E-GMA (70/20/10, w/w) blend. These blends were also annealed for 48 h at 80°C, but annealing resulted in decreases in both impact strength and elongation at break. Going one step further, quaternary blends were produced with the addition of polycarbonate (PC). For PLA/PC/SEBS/E-GMA (40/40/15/5, w/w) blends, the heat deflection temperature and aging resistance were improved, but the notched impact strength was decreased compared to the notched impact strength of the ternary blends. Jiang *et al.* indicated that injection-molded PLA/E-GMA blends exhibit a fine co-continuous microlayer structure leading to high toughness and low linear thermal expansion.[16] In that study, E-GMA was compared with maleic anhydride grafted poly(styrene-ethylene/butylene-styrene) triblock elastomer (*m*-SEBS), and poly(ethylene-*co*-octene) (EOR).

As aforementioned, both blending and addition of rigid fillers have some drawbacks. Thus, some researchers are trying to balance the effects of flexible polymers and rigid fillers by producing ternary composites.[17–22] Chen *et al.*[17] produced PLA/PBS/C25A nanocomposites. Upon addition of 10 wt % C25A to the blend of PLA/PBS (75/25, w/w) the tensile modulus increased from 1.08 to 1.94 GPa, but the elongation at break decreased from 71.8% to 3.6% which was even lower than the elongation at break of the neat PLA that was used. The use of an epoxy-functionalized organoclay (TFC) instead of C25A at the same content resulted in the same level of tensile modulus, and the elongation at break increased to 118%.

A core–shell rubber impact modifier Paraloid^{TM} EXL 2330 was used in PLA/clay/core–shell rubber ternary composites by Li *et al.*[18] With the addition of 20 wt % EXL 2330 and 5 wt % C30B clay, the notched Izod impact strength increased to 5.2 kJ/m^2 from the value of 2.2 kJ/m^2 for neat PLA. Also, in the same nanocomposite, 1% decrease in tensile modulus was accompanied by a 40% decrease in tensile strength. Jiang *et al.*[23] compared the effects of organically modified montmorillonites (OMMT) and nano-sized precipitated calcium carbonate (NPCC) on the mechanical properties of PLA and poly(butylene adipate-*co*-terephthalate) (PBAT) blends. Higher tensile strength and modulus were obtained with the composites containing OMMT, but the elongation at break of these nanocomposites was lower compared to the elongation at break of the nanocomposites containing NPCC. In the same study, by replacing 25 wt % of the PLA with maleic anhydride grafted PLA (PLA-*g*-MAH), significant increases were obtained in the elongation at break. This could be attributed to the improved surface interactions in the presence of maleic anhydride functional groups. Most recently, in our previous study, rubber-toughened PLA nanocomposites prepared by melt blending were investigated focusing on blending order of the components.[24] Those nanocomposites were prepared with a single OMMT type (C30B) and at a single OMMT content (2 wt %) with varying ethylene-methyl acrylate-glycidyl methacrylate (E-MA-GMA) copolymer content. Intercalated/exfoliated structures were obtained for rubber contents of 10 wt % and higher. In addition to this, the best balance of these mechanical properties was obtained at 10 wt % rubber content.

In this study, using a constant filler loading and the optimum rubber content reported in our previous study[24] different rubber and clay modifier combinations were investigated. To investigate the effects of different nanoclay types, five commercial organically modified nanoclays (Cloisites®15A, 25A, and 30B, and Nanofils®5 and 8) were loaded to PLA matrix. Two elastomers, ethylene-glycidyl methacrylate (E-GMA) and ethylene-butyl acrylate-maleic anhydride (E-BA-MAH), were used as the impact modifiers that also acted as compatibilizers. The nanocomposites were produced by melt compounding. The morphological structures of the nanocomposites were investigated using XRD, SEM, and TEM. The mechanical performances of the nanocomposites were evaluated by impact and tensile tests.

EXPERIMENTAL

Materials

As the polymer martix, a transparent, injection molding grade PLA (ca. 5% D-lactide) with weight average molecular weight (M_w) of 278,000 and polydispersity (M_w/M_n) of 1.78 was purchased from NaturePlast (France). Lotader® AX8840, a copolymer

of ethylene (E) and glycidyl methacrylate (GMA); and Lotader 2210, a terpolymer of ethylene (E), butyl acrylate (BA), and maleic anhydride (MAH) was purhased from Arkema Chemicals (France) and used as impact modifier-compatibilizer. Five different organically modified montmorillonites: Cloisites®15A (C15A), 25A (C25A), and 30B (C30B), and Nanofils®5 and 8 (N5 and N8) were purchased from Southern Clay Products. Organic modifier of C15A, N5, and N8 contains dimethyl, dihydrogenated tallow, quaternary ammonium cation, and chloride anion. According to the manufacturer, the main differences between these OMMTs are the modifier contents and *d*-spacing values. The organic modifier of C25A is dimethyl, dehydrogenated tallow, 2-ethylhexyl quaternary ammonium cation (2MHTL8) with methyl sulfate anion. The organic modifier of C30B is methyl, tallow, bis-2-hydroxyethyl quaternary ammonium (MT2EtOH) with chloride anion.

Nanocomposite and Sample Preparation Methods

All nanocomposites and blends were prepared by extrusion using a co-rotating, intermeshing twin screw extruder (Thermoprism TSE 16 TC) with dimensions of $L = 384$ mm and $D = 16$ mm. The barrel temperature and the screw speed were 170°C and 250 rpm, respectively. Before extrusion, all the raw materials were dried in a vacuum oven at suitable temperatures. PLA and OMMTs were dried at 85°C, and E-GMA and E-BA-MAH were dried at 70°C. After the extrusion step, the extrudate was cooled below its glass transition temperature on a specially designed cooling band with a length of 120 cm that carried the extrudate. Cooling process was accelerated using a compressor blowing air onto the band. Cooled strips of polymer composites were pelletized in a grinder. The pellets obtained at the end of the process were stored in desiccators to prevent probable hydrolysis due to contact with the moist air. Before all molding and/or characterization processes, the composites were dried overnight under vacuum at 80–85°C. To have a reference material, neat PLA was also melt-processed under identical extrusion conditions. Compatibilizer and nanoclay contents were kept constant at 10 wt % and 2 wt %, respectively, to monitor the effects of their chemical structures.

Melt processed nanocomposites were injection molded using a laboratory scale injection-molding machine (DSM Micro 10 cc Injection Molding Machine) and the samples were used for analyses of morphology and mechanical tests. The barrel and mold temperatures of injection molding device were adjusted as 170°C and 55°C, respectively, and the maximum pressure during molding was 12 bars.

Characterization Methods

X-ray Diffraction. X-ray diffraction (XRD) patterns of pure organoclays and injection molded nanocomposites were obtained using Rigaku Ultima-IV X-ray diffractometer that generated a voltage of 40 kV and current 40 mA from CuKα radiation source ($\lambda = 1.5418$ Å). The diffraction angle, 2θ, was scanned from 1° to 10° with a scanning rate of 1°/min and a step size of 0.01°.

Scanning Electron Microscopy. Scanning electron microscopy (SEM) analysis was performed with Quanta 400F Field Emission Microscope. SEM images were taken for each specimen at 500× and 3000× magnifications. For the nanocomposites without a rubbery phase, SEM images are used to investigate the fracture mechanism. For the nanocomposites containing a rubbery phase, the fractured surfaces of the samples were etched with *n*-heptane at 60°C in a constant temperature water bath using ultrasonication. Etching was applied to remove the elastomeric phase on the surface so that the domain size analyses would be easier. The average size of the dispersed phase was analyzed using Image J software program on at least for 1000 different rubber domains. At least three images with a magnification of 3000× were analyzed. The area of each hole in the samples was determined using the image analysis software by transforming these black holes into ellipsoids and calculating the area of these ellipsoids. Then, the average domain size (average diameter) was calculated statistically by the box plot method.

Transmission Electron Microscopy. The spatial distribution of nano-sized fillers was examined using high-resolution transmission electron microscopy (FEI, Tecnai G2 F30), operated at an accelerating voltage of 300 kV. For TEM imaging, ultrathin sections (~120 nm) were prepared from injection molded samples by cryogenic ultramicrotome (Leica, EMFC6), that was operated at $T = -80$°C.

Fourier Transform Infrared Spectroscopy. FTIR was used for investigating PLA-compatibilizer interactions. FTIR analyses of the nanocomposites were performed in attenuated total reflectance (ATR) mode. No preliminary treatments were done on the samples cut from injection molded samples.

Mechanical Properties. Tensile tests were performed according to ISO 527 with Shimadzu AG-IS 100 kN test machine at a strain rate of 0.1 min^{-1}. Unnotched charpy impact tests were performed using Ceast Resil Impactor on samples with dimensions of 80 × 10 × 4 mm^3 according to ISO 179. All the tests were performed at room temperature, and all the results are the averages of five samples.

RESULTS AND DISCUSSION

XRD and TEM

X-ray diffractograms are widely used to assess the dispersion of layered silicates in the polymer matrix. In fact, the peaks on the diffractograms between $2\theta = 1$–10° illustrate the layer spacing of the nanocomposites. In this range, PLA and the copolymers used to toughen PLA (E-GMA and E-BA-MAH) do not show any peaks. For easier comparison, the XRD pattern of the pure clay is shown at the top of each subfigure in Figure 1. For both binary and ternary compositions, there is a large peak at low 2θ values that corresponds to the silicate layers intercalated by the polymer chains. The second peak seen at higher 2θ values is attributed to the second registry due to the diffraction from d_{002} plane.[6,25] In Table I, the interlayer spacing values calculated using Bragg's law from the first characteristic peaks are summarized. When the changes in the interlayer with respect to the pure OMMT are considered, the highest changes are observed for C25A and C30B, which is consistent with the findings in the literature.[5,26] The differences in the compatibilizing effects of the elastomers are also shown by the diffractograms. Ternary nanocomposites containing E-GMA as the rubbery phase

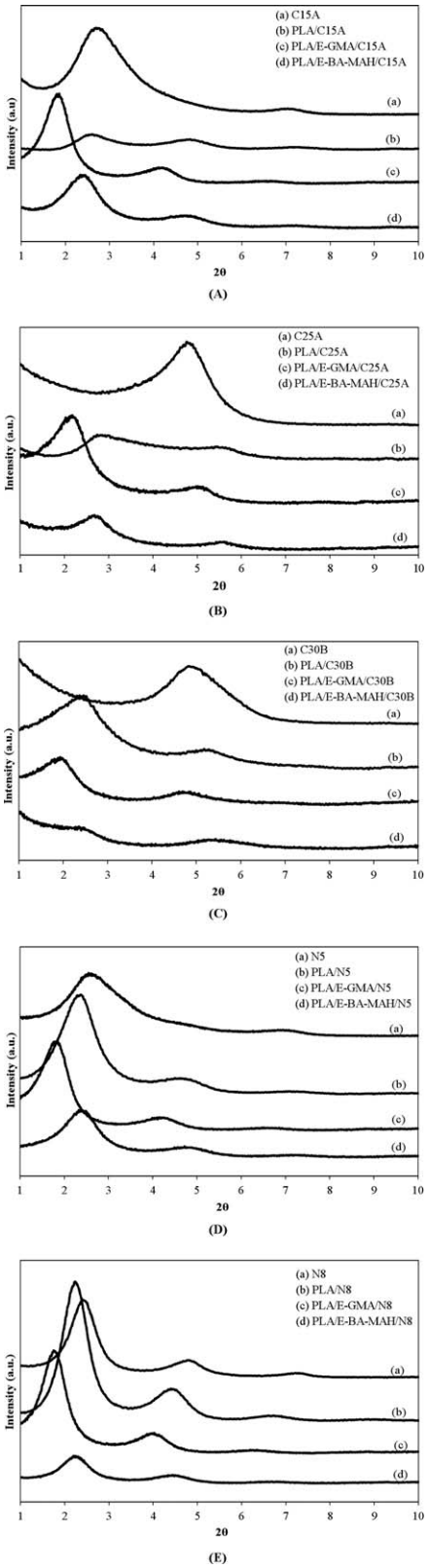

Figure 1. XRD patterns of PLA nanocomposites filled with different OMMTs: (A) C15A, (B) C25A, (C) C30B, (D) N5, and (E) N8.

resulted in at least 20% increase in interlayer distance (PLA/E-GMA/C30B) as compared to unprocessed OMMT. This increase reaches to 35% for PLA/E-GMA/C15A. Conversely, ternary nanocomposites containing E-BA-MAH as the rubbery phase do not show a significant change in terms of interlamelar distances compared to the samples containing neither of the rubbers. This is probably due to better polarity matching between GMA as a functional group with the organic modifiers and the polmer matrix. Among the Cloisites®, C30B has the lowest hydrophobicity. C15A has the highest hydrophobicity, and it results in the lowest degree of intercalation according to the XRD patterns. In addition, XRD patterns of the nanocomposites containing C15A, N5, and N8 follow similar trends with each other. These three nanoclays contain modifiers with the same chemical structure, and the changes in the gallery height of the nanocomposites containing either of these clay types are lower than the other two.

The XRD patterns provide valuable information about the distribution of the filler in the matrix, but the information on the spatial distribution of clay nano-particles can be visualized only by TEM.[27,28] Two binary nanocomposites and two ternary nanocomposites containing E-GMA as the rubbery phase were analyzed by TEM. Ternary nanocomposites containing E-BA-MAH were left out of the scope, since according to the XRD patterns, they display no enhancement in dispersion of clay and intercalation/exfoliation mechanisms. Figure 2 shows the TEM images of PLA/C25A binary nanocomposite and PLA/E-GMA/C25A ternary nanocomposite at different magnifications. It is possible to see three different states of dispersion of the clay nanoplatelets in both nanocomposites. The interlayer spacing between the intercalated layers of PLA/C25A is measured using Image J, and is in accordance with the XRD results (~3.2 nm). According to the XRD analyses, addition of E-GMA to the binary PLA/C25A nanocomposite resulted in an increase in the interlayer spacing. TEM images reveal that there are tactoids together with some intercalated and orderly exfoliated silicate layers. The contrast difference between the polymer matrix and the rubbery phase is not enough to differentiate between these two constituents in the micrographs preventing the elaboration on positions of clay nanoplatelets. In melt processing, the rubber is melted before PLA as its melting point is lower. Because of this difference, fillers might be encapsulated in the rubber before PLA melts, or they might just reside on the interface between the PLA matrix and the rubber domains.[28]

As suggested by the XRD results, increases in interlayer spacing of C15A, N5, and N8 are smaller compared to those of C25A and C30B, in both binary and ternary nanocomposites. To represent these three clay types, N5 nanocomposites were analyzed by TEM.

Table I. Interlayer Spacing Values of Pure OMMTs and Nanocomposites Calculated Using XRD Patterns

Sample	C15A	C25A	C30B	N5	N8
Pure OMMT	33.1 Å	18.3 Å	18.1 Å	34.2 Å	36.1 Å
PLA/OMMT	35.3 Å	31.9 Å	37.2 Å	37.4 Å	38.9 Å
PLA/E-GMA/OMMT	47.9 Å	40.3 Å	44.6 Å	48.2 Å	49.5 Å
PLA/E-BA-MAH/OMMT	36.7 Å	33.5 Å	35.6 Å	38.8 Å	39.4 Å

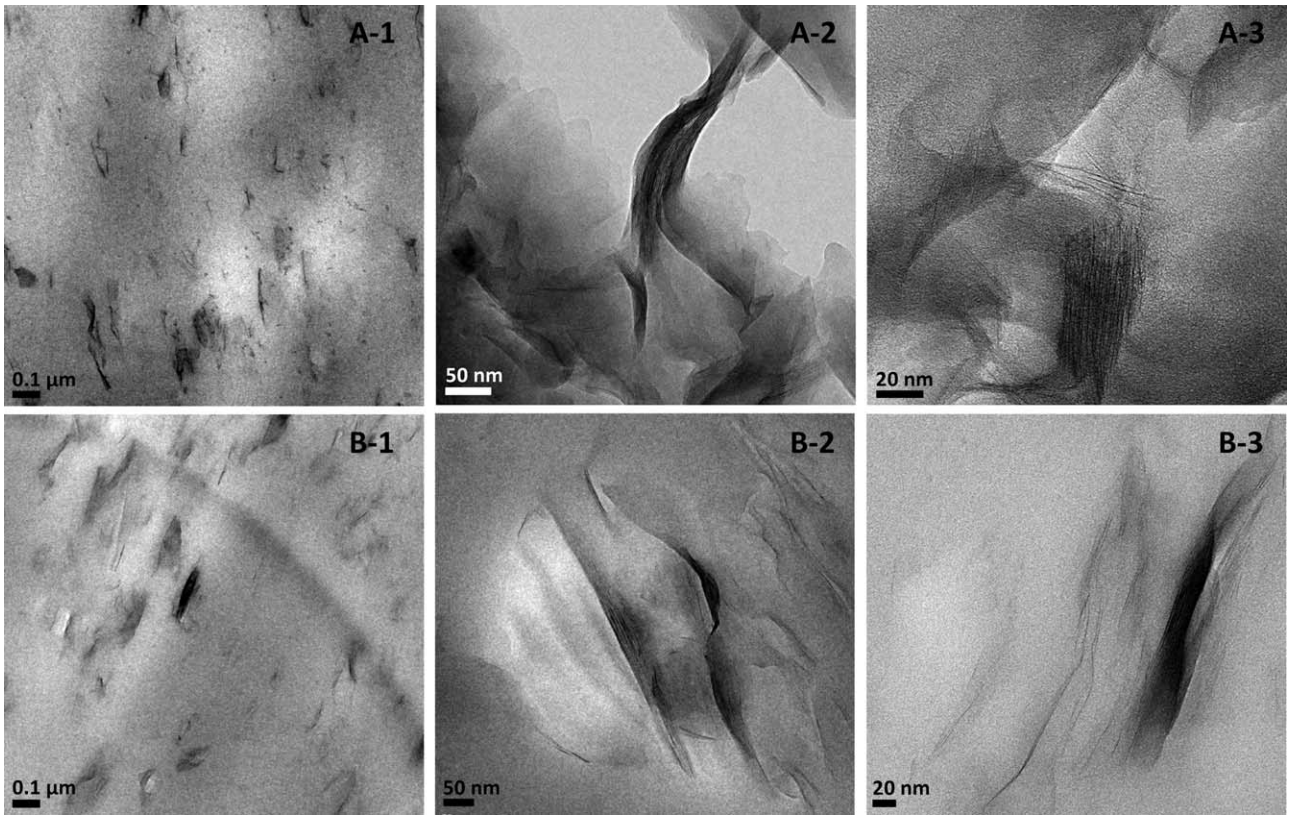

Figure 2. TEM micrographs of the nanocomposites containing 2 wt % clay: (A) PLA/C25A; (B) PLA/E-GMA/C25A.

Figure 3 shows the TEM micrographs of PLA/N5 binary nanocomposite and PLA/E-GMA/N5 ternary nanocomposite at different magnifications. Different states of dispersion can be seen as in the case of C25A binary nanocomposite. The layer spacings, determined by the same image analysis software, are consistent with the XRD analyses. Intercalated structures in PLA/N5 have interlayer spacing of about 3.7 nm according to the XRD analyses and in the high magnification micrographs, gallery heights varying between 3.5 and 4.0 nm were detected for the same nanocomposites.

Scanning Electron Microscopy

The main limitation in PLA applications is its inherent brittleness. As expected in a brittle polymer, the impact fracture surface of PLA exhibits straight crack propagation lines [Figure 4(A)]. These straight lines grow rapidly and make it easier to fracture the specimen with a small amount of energy. PLA/OMMT nanocomposites have fracture surfaces that are similar to that of neat PLA [Figure 4(B–F)]. Most of the crack propagation lines are distinct and long, but the fracture surfaces are rougher compared to that of neat PLA. There are smaller cracks that are developed in various directions. The results of mechanical property investigations will be discussed in the forthcoming sections, but it can be stated here that addition of nanofillers did not result in considerable enhancement in impact toughness compared to the impact strength of neat PLA. The addition of organoclays deflected the cracks and increased their path to some extent, but they did not act as barriers to stop crack propagation.

Blending PLA with rubbers resulted in phase separated morphologies for both E-GMA and E-BA-MAH (Table II). Sizes of the rubbery domains of these two blends are considerably different [Figures 5(A) and 6(A)]. The average domain sizes of PLA/E-GMA and PLA/E-BA-MAH blends are 714 and 1023 nm, respectively. In addition to the chemical interactions between the polymer matrix and the rubbers, the viscosity difference in different rubbers might result in different coalescence mechanisms. The viscosity of E-BA-MAH is slightly higher than the viscosity of E-GMA which probably prevents the elastomeric phase E-BA-MAH to disperse into small droplets.

As the fracture surfaces of ternary nanocomposites are etched, and etching annihilates the crack propagation lines, detailed fracture mechanisms cannot be given. However, the phase separation between the polymer matrix and the compatibilizer, and the dispersion of the rubbery phase in the matrix can be investigated. Size and shape of spherical vacuoles that remained after etching reveal the distribution of the rubbery domains, which is an indication of the stability of the system. In the samples containing E-GMA, narrow size distribution of the dispersed phase with sub-micron sizes could be attributed to the compatibility of the phases with low interfacial tension and the achievement of efficient reactive blending.

Increased domain sizes in the nanocomposites containing C25A and C30B could be attributed to the positions of the clay nanoplatelets in the nanocomposite. If the organoclay particles are dispersed in the PLA matrix, the clay platelets suppress the

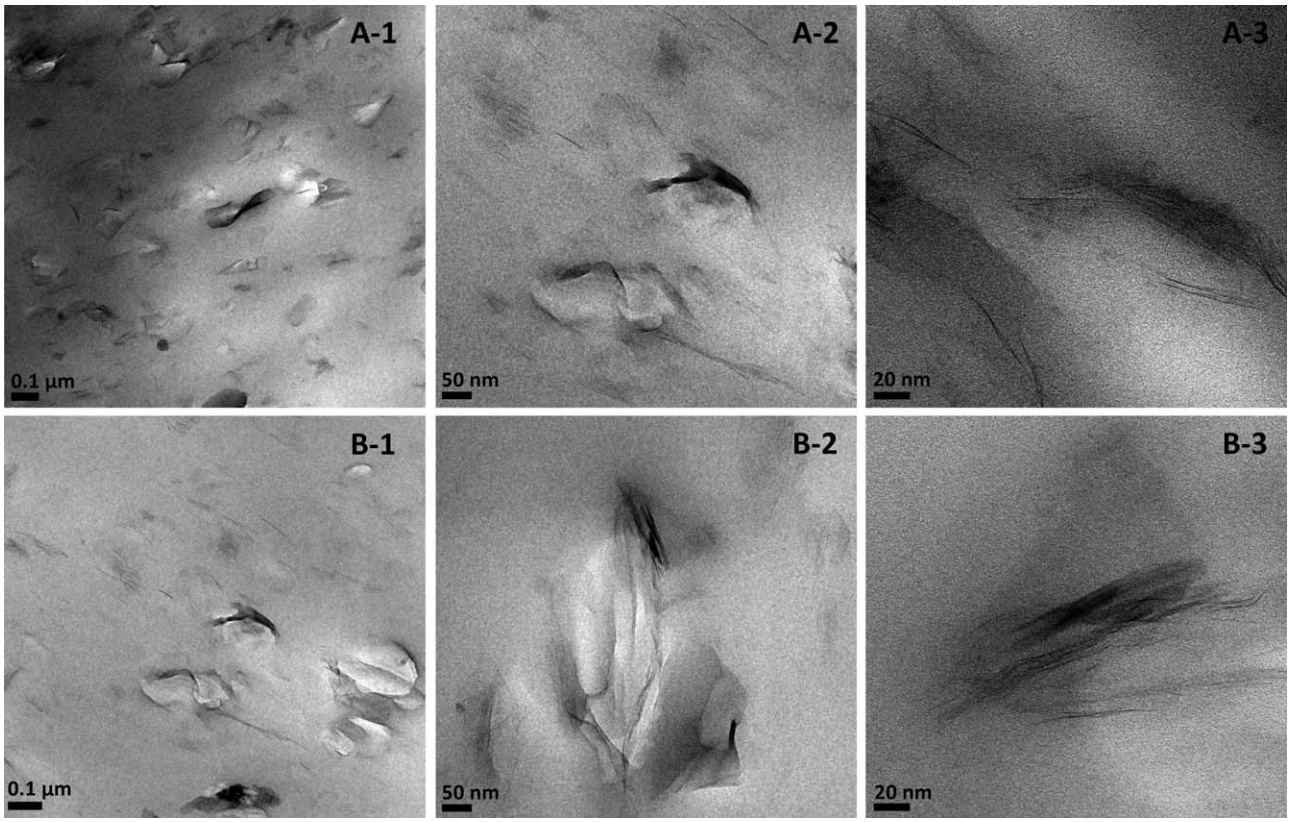

Figure 3. TEM micrographs of the nanocomposites containing 2 wt % clay: (A) PLA/N5; (B) PLA/E-GMA/N5.

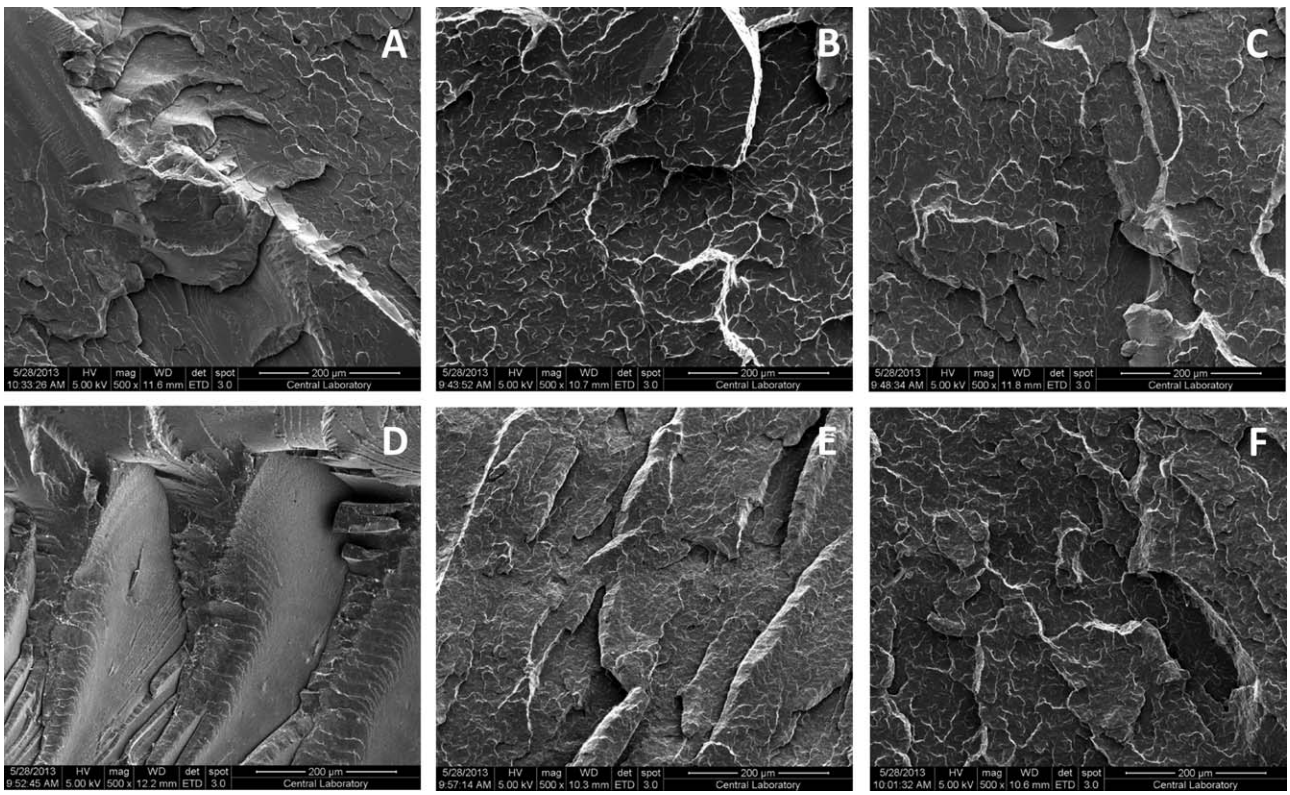

Figure 4. SEM micrographs: (A) Neat PLA, (B) PLA/C15A, (C) PLA/C25A, (D) PLA/C30B, (E) PLA/N5, and (F) PLA/N8.

Table II. Sizes of Rubber Domains Determined from SEM Images

Rubber type	Clay type	d_{av} (nm)
E-GMA	–	714
E-BA-MAH	–	1023
E-GMA	C15A	547
E-GMA	C25A	732
E-GMA	C30B	792
E-GMA	N5	540
E-GMA	N8	573
E-BA-MAH	C25A	1255
E-BA-MAH	N5	1146

agglomeration of the elastomeric domains and cause a barrier effect that hinders the recombination of elastomeric domains.[29] However, for C25A and C30B, the average domain sizes increase with the addition of organoclay indicating that these clay particles have a tendency to reside at the interphase between the PLA and elastomeric material, and thus the interfacial tension is reduced and the domain sizes are enlarged. Ternary nanocomposites of C15A, N5, and N8 with the compatibilizer E-GMA resulted in smaller domain sizes compared to those of PLA/E-GMA binary blend. Smaller domain sizes might be an indication of dispersion of the clay nanoparticles in the PLA polymer matrix suppressing the rubber droplets. However, these results show that none of the morphology analyses directly indicate the position of clay nanoplatelets, but they just show evidence supporting the possibilities of being located at the interface between the two phases or being embedded in the rubber phase.

Nanocomposites containing E-BA-MAH were analyzed by SEM, only for C25A and N5 containing samples (Figure 6). Similar to the observation in the binary blends, E-BA-MAH containing nanocomposites have larger rubber droplets than their equivalent samples prepared with E-GMA. For E-BA-MAH containing nanocomposites, large domains are attributed to weaker compatibility of maleic anhydride functional group with PLA, as compared to epoxide functional group with PLA. The difference in the morphologies of E-GMA and E-BA-MAH containing nanocomposites is reflected in both mechanical and rheological properties, and the latter is discussed in another publication.[30] In that study, the apparent shear-thinning observed in PLA-organoclay nanocomposites containing E-BA-MAH was attributed to weaker interactions between MAH and PLA, as compared to GMA and PLA.

FTIR

The bands that are expected in the infrared spectra of PLA are well stated in the literature.[31,32] The interactions between the compatibilizers and the polymer matrix can be followed through the changes in the FTIR spectra of the blends and nanocomposites. As an example, FTIR spectra of the nanocomposites of C25A with and without compatibilizers, together with neat PLA, neat E-GMA, and neat E-BA-MAH, are shown in Figure 7. The reaction that is expected to occur between the

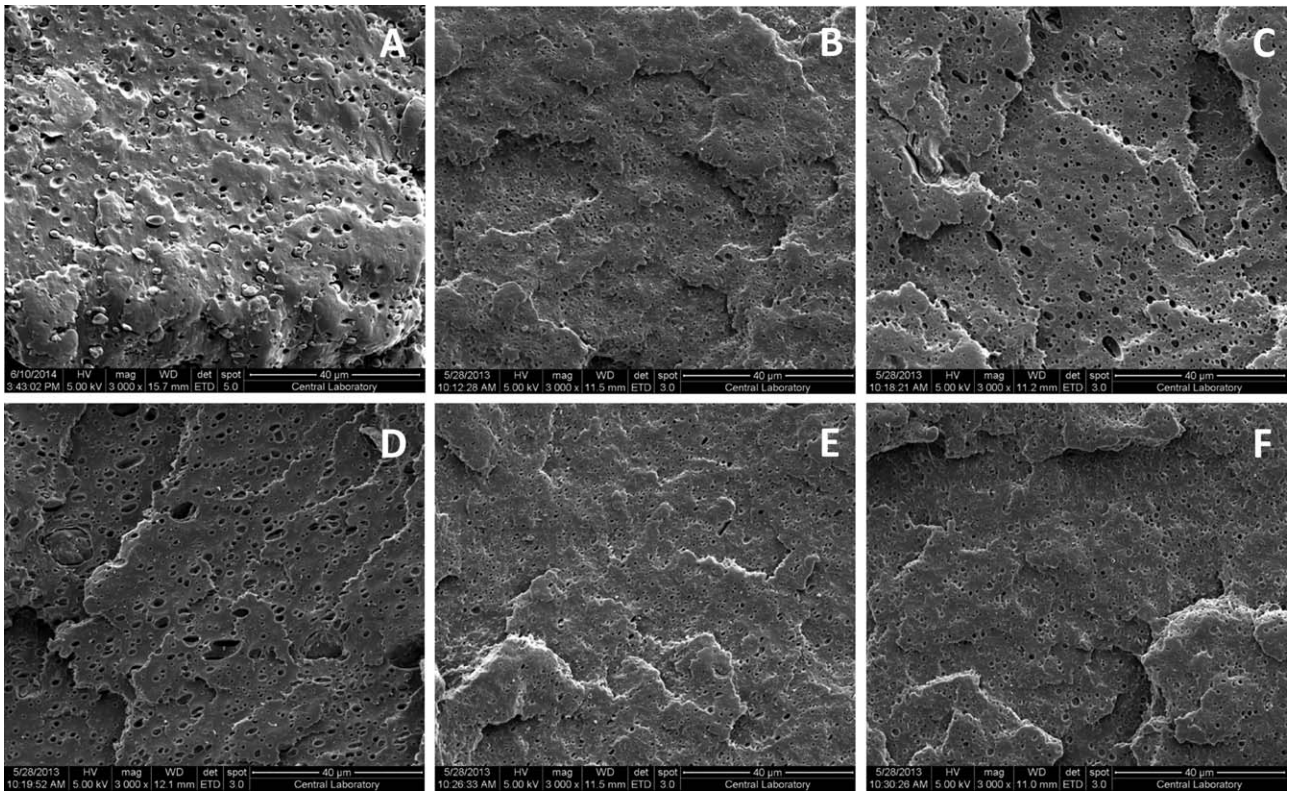

Figure 5. SEM micrographs: (A) PLA/E-GMA, (B) PLA/E-GMA/C15A, (C) PLA/E-GMA/C25A, (D) PLA/E-GMA/C30B, (E) PLA/E-GMA/N5, and (F) PLA/E-GMA/N8.

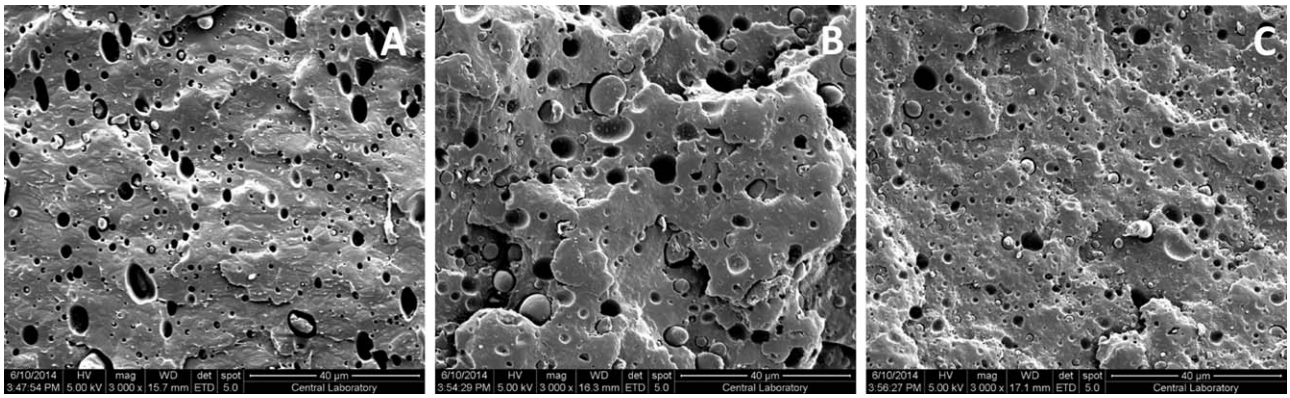

Figure 6. SEM micrographs: (A) PLA/E-BA-MAH, (B) PLA/E-BA-MAH/C25A, and (C) PLA/E-BA-MAH/N5.

end groups of PLA (—COOH and/or —OH) and the epoxide group of E-GMA can be detected from the decreasing intensity or disappearance of the epoxide peak seen at 910 cm^{-1} in the FTIR spectra of neat E-GMA.[32,33] Similarly, the reaction between PLA end groups and maleic anhydride functional group of E-BA-MAH can be observed from the decreasing intensity or disappearance of the maleic anhydride peak seen at 1785 cm^{-1}.[32,34] Both of these characteristic peaks disappeared in the spectra which could be analyzed in two ways. The elastomers could have interacted with PLA during melt blending so that both epoxide and maleic anhydride peaks disappeared in the spectra of the corresponding ternary nanocomposites. Another possibility is that the intensity of those peaks was too low to be detected when the elastomer content is 10 wt %.

Mechanical Properties

Consistent with the expectations, addition of the compatibilizers resulted in lower tensile strength and modulus values (Figures 8 and 9) in comparison to the properties of neat PLA. Both of the binary blends have the same tensile strength and comparable modulus values that are lower than the strength and modulus values of neat PLA. PLA/organoclay binary nanocomposites resulted in reduction of tensile strength as compared to the tensile strength of neat PLA, with the maximum reduction of 34% in the PLA/N8 nanocomposite. In most studies, addition of nanofillers results in an enhancement in tensile strength. The reason of the reduction observed in this study might be the weak spots in the matrix that exist due to the clay agglomerates in the non-compatibilized samples. Compatibilization, conversely, resulted in higher tensile strength with the addition of nanoclay. For example, drastically decreased strength of the PLA/E-GMA blend was improved up to 3.3-fold with the addition of nanofillers in the PLA/E-GMA/N5 nanocomposite. Similar tensile strength reductions in binary nanocomposites, and improvement in ternary nanocomposites, were recently reported in the literature.[22,28] Nanocomposites containing E-BA-MAH also showed tensile strength improvement with the addition of organoclay, but these enhancements are very low compared to the increase in the samples containing E-GMA.

Owing to the elastomeric nature of the rubbers, modulus values of the blends are lower than that of neat PLA. Blending with 10 wt % E-GMA or E-BA-MAH caused 37% and 30% reductions, respectively, in the tensile modulus. These reductions are a little higher than the ones observed in similar studies published in the literature.[14] In the binary nanocomposites, enhancement in modulus was seen only with C25A and C30B, while the other clay types resulted in slight decreases in the modulus. These two

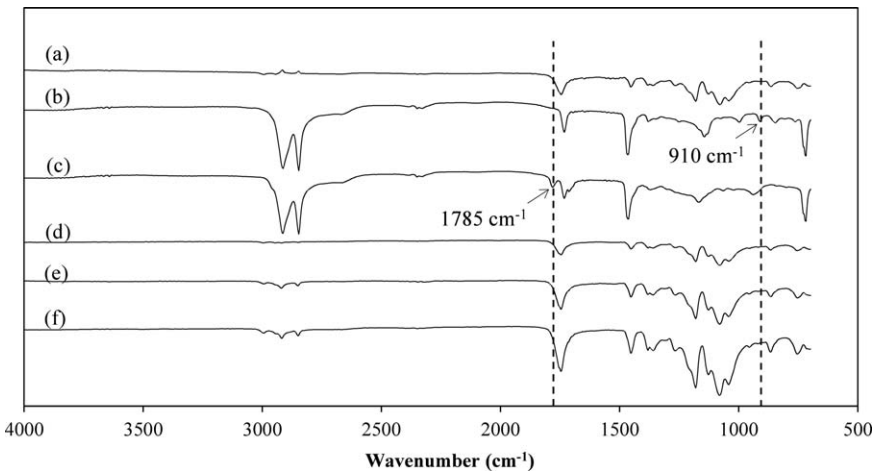

Figure 7. FTIR spectra of (a) PLA, (b) E-GMA, (c) E-BA-MAH, (d) PLA/C25A, (e) PLA/E-GMA/C25A, and (f) PLA/E-BA-MAH/C25A.

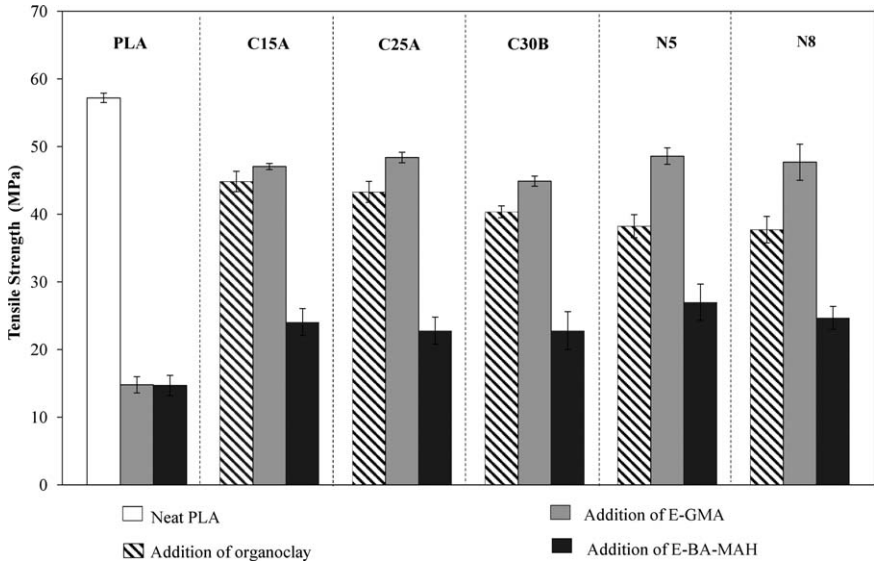

Figure 8. Effects of the types of organoclay and compatibilizer on tensile strength.

types of clays were previously used in the literature with PLA as the polymer matrix. Affinity of C30B has shown to be higher than that of C25A due to hydrogen-bonding between the carbonyl group in the PLA structure and the hydroxyl group in the organic modifier of 30B,[6,35,36] although enhancement of modulus of C25A is slightly higher in this study. Furthermore, as compared to C15A, C25A has also shown to have higher affinity to PLA.[5] According to the manufacturer, C15A, N5, and N8 contain similar organic modifiers, and the main differences between them are the modifier content and *d*-spacing values. According to the XRD patterns, low affinity of these clay types to PLA resulted also in low degree of intercalation. Thus, dispersion of the filler and mechanical properties are highly affected by the intermolecular affinities of the organic modifier with the polymer matrix even at low concentrations, that is, 2 wt %.

The positive effect of addition of nanofiller on the tensile modulus is clear in the ternary nanocomposites. Modulus reductions due to blending are highly compensated with the addition of 2 wt % organoclay for each sample. This is due to the stiffening effect of the clay nanoplatelets that promotes chain immobilization.[21,22,37,38]

The most interesting results obtained from the tensile tests are probably the elongation at break values. Neat PLA is known to elongate not more than 10% indicating that it is hard and brittle. Figure 10 shows the changes in elongation at break of binary blends, and binary and ternary nanocomposites. Blending with E-GMA resulted in almost eightfold increase in elongation at break. However, blending with E-BA-MAH caused reduction in elongation at break. Ternary nanocomposites containing E-BA-MAH also failed at very low elongations, such that all these nanocomposites failed at a lower percent elongation value as

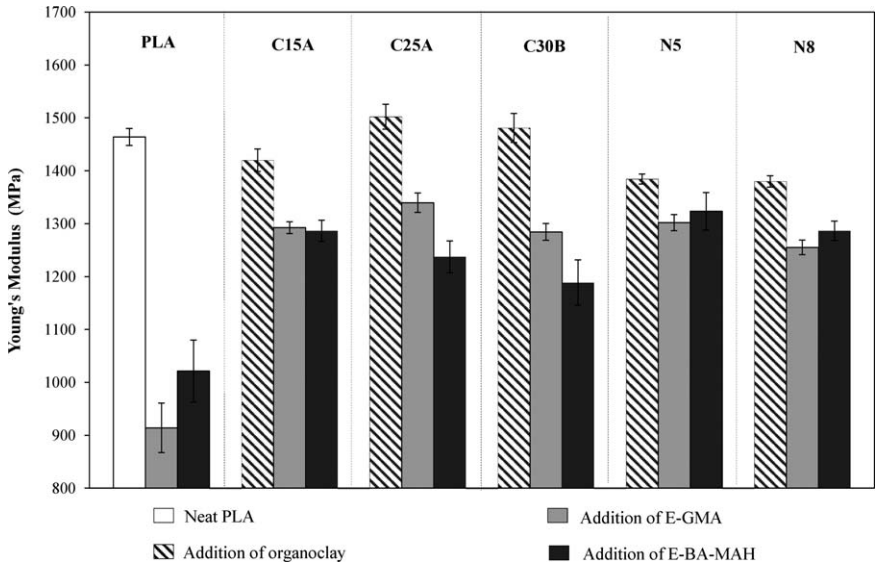

Figure 9. Effects of the types of organoclay and compatibilizer on Young's modulus.

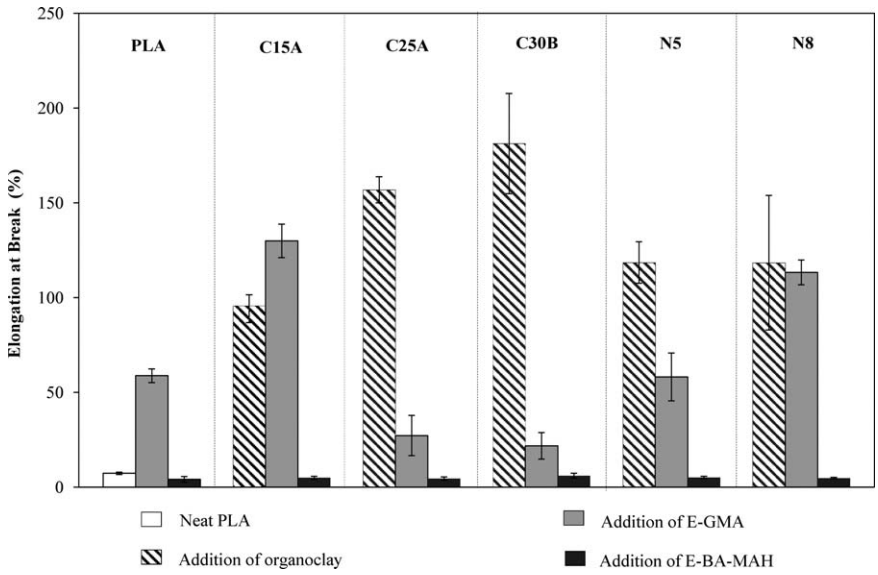

Figure 10. Effects of the types of organoclay and compatibilizer on elongation at break.

compared to the elongation at break of neat PLA. Peterson *et al.*[38] also reported decreases in elongation at break of PLA/organically modified layered silicates with the addition of maleic anhydride grafted PLA (PLA-MA) to the nanocomposites. SEM images of the PLA/E-BA-MAH binary blend and the PLA/E-BA-MAH/organoclay nanocomposites showed considerably larger rubber droplets in their structure compared to the samples containing E-GMA as rubber. Average droplet sizes of E-BA-MAH containing samples are almost 1.4-fold larger than the ones containing E-GMA. Domain sizes should be optimum in applications, as both too small and too large domains can affect the final mechanical properties adversely. If the two phases are highly compatible, ultra-fine domains could be formed. Finely distributed tiny domains might result in low impact strength values, as these domains cannot act as barriers for the cracks, and the cracks can propagate without touching the rubbery phases. Conversely, too large domains can form large cavities when they are deformed.[39]

It is well known that the addition of stiff reinforcements can reduce the elongation at break of the matrix, because the reinforcements would cause stress concentrations. However, this is not the case in PLA/organoclay nanocomposites produced in this study. All clay types increased the percent elongation at break, even at higher levels than blending PLA with E-GMA. For PLA/organoclay nanocomposites, increases in elongation at break values are also reported in the literature.[40] Up to a certain loading, both the small clay tactoids and the exfoliated/intercalated structures can be aligned during injection molding and also during tensile testing. This alignment in the direction of extension may also help distribution and transfer of load between the matrix and the filler, resulting in an increase in elongation at break. However, at higher filler contents, mobility of the constituents might decrease, causing a reduction in elongation at break. For the samples in which E-GMA is used as the rubbery phase, the elongation at break of the samples

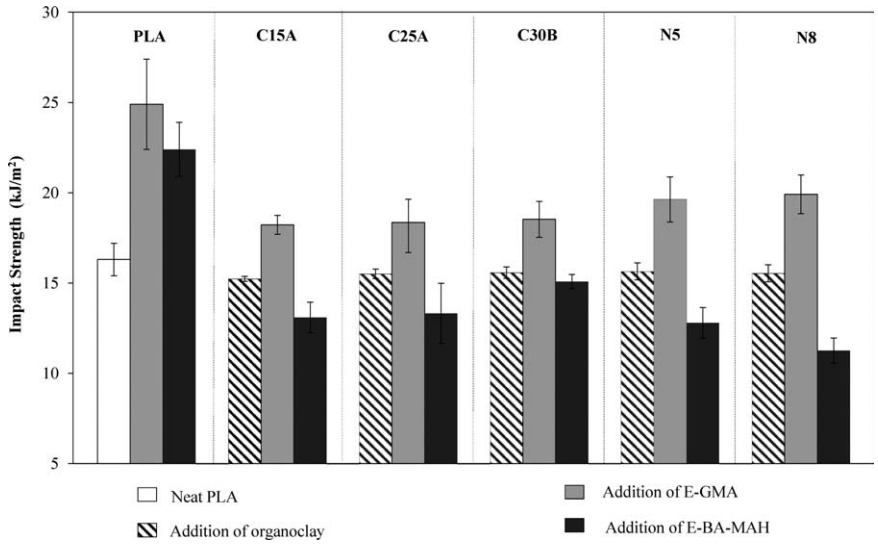

Figure 11. Effects of the types of organoclay and compatibilizer on impact strength.

containing C15A, N5, and N8 is significantly higher than the elongation at break of nanocomposites with other clays. XRD patterns of E-GMA containing ternary nanocomposites showed that C25A and C30B displayed high degrees of intercalation. Additionally, SEM micrographs of these nanocomposites suggest that, in these nanocomposites clay nanoplatelets are more probably located at the interface between the matrix and the rubber droplets. This might prevent the alignment of the silicate layers in the direction of extension, lowering the final elongation at break.

Unnotched Charpy impact strength of neat PLA, PLA binary blends, and PLA nanocomposites are shown in Figure 11. The unnotched impact strength is a measure of the energy to initiate and propagate a crack, in other words resistance to crack initiation and propagation.[41] Incorporation of 2 wt % clay into the polymer matrix caused a minor decrease in the impact strength, independent of the type of clay. SEM images of the binary nanocomposites displayed smaller cracks compared to that of impact fractured neat PLA surface. However, as discussed before, deflection of the cracks obviously did not act as barriers to stop crack propagation and did not increase the energy absorbed.

The binary blends reached the highest impact strength values such that blending with E-GMA and E-BA-MAH resulted in increases of 1.5- and 1.4-fold compared to the impact strength of neat PLA. Impact strength values of ternary nanocomposites containing E-GMA are all higher than that of neat PLA, but lower than that of the binary PLA/E-GMA blend. The impact strength values of the nanocomposites containing E-BA-MAH are lower than that of PLA/E-BA-MAH blend and neat PLA. The improvement of impact strength by blending with block copolymers is directly related to the size of the dispersed elastomeric domains in the polymer matrix. Usually, as the domain size increases the impact strength increases owing to lower stress concentration effect of the domains. However, the domain size should not be too high, as large domains form large cavities that join rapidly and cause failure of the specimen. Image analyses of SEM micrographs showed that the droplets E-BA-MAH are 1.4-fold larger than E-GMA droplets. This difference in rubber domain sizes and the incompatibility of E-BA-MAH with PLA, as observed in almost all the material properties, are the main reasons of reduction of impact strength values in samples containing E-BA-MAH.

CONCLUSIONS

It was observed that even at low clay loadings the structure of modifier influences the nanocomposite properties. Dispersion of clay in the PLA matrix was highly affected by the type of the organic modifier of the clay. Even though nanocomposites exhibited both intercalated and some exfoliated layers with some remaining tactoids, the degree of intercalation was determined by the chemical compatibility between the polymer matrix and the modifier. Compatibilizer structure is another important parameter affecting the final morphology. Good polarity matching between the modifier structures of C25A and C30B and the compatibilizer E-GMA resulted in high degree of intercalation. This phenomenon was coupled with the high reactivity of the epoxide group of GMA towards the end groups of PLA as compared to the MAH functional group. Even though SEM images of two compatibilizers exhibited different structures, the reactive interaction between both rubbers and the polymer matrix was proven by the FTIR results. The copolymer formed at the interface of the two phases, as a result of the reaction that occurred during extrusion, acted as a bridge transferring the load and increasing the toughness. Furthermore, ellipsoidal shape of the vacuoles that remained on the fracture surface indicates that there was good interaction between the dispersed phase and the matrix such that the impact load was shared between the phases especially for the case of E-GMA. Effects of the changes in the microstructure were reflected in the mechanical properties. Both of the binary blends had tensile strength and modulus values that were lower than those of the neat PLA, and tensile strength and modulus were compensated to a certain extent in the ternary nanocomposites. Increases in elongation at break, which could be an indication of tensile toughness, were mostly apparent for PLA/E-GMA blend and PLA/OMMT binary nanocomposites. Impact toughening could be achieved for binary blends and ternary nanocomposites containing E-GMA as the rubber.

REFERENCES

1. Liu, H.; Zhang, J. *J. Polym. Sci., Part B: Polym. Phys.* **2011**, *49*, 1051.
2. Auras, R.; Harte, B.; Selke, S. *Macromol. Biosci.* **2004**, *4*, 835.
3. Inoh, T.; Kageyama, T. *SAE Tech. Paper 2003-01-2756*, **2003**, doi:10.4271/2003-01-2756.
4. Sinha Ray, S.; Bousmina, M. *Prog. Mater. Sci.* **2005**, *50*, 962.
5. Krikorian, V.; Pochan, D. J. *Chem. Mater.* **2003**, *15*, 4137.
6. Pluta, M.; Paul, M.-A.; Alexandre, M.; Dubois, P. *Polym. Sci., Part B: Polym. Phys.* **2005**, *44*, 299.
7. Anderson, K. S.; Lim, S. H.; Hillmyer, M. A. *J. Appl. Polym. Sci.* **2003**, *89*, 3757.
8. Wang, L.; Ma, W.; Gross, R. A.; McCarthy, S. P. *Polym. Degrad. Stabil.* **1998**, *59*, 161.
9. Semba, T.; Katigava, K.; Ishiaku, U. S.; Hamada, H. *J. Appl. Polym. Sci.* **2006**, *101*, 1816.
10. Takayama, T.; Todo, M. *J. Mater. Sci.* **2006**, *41*, 4989.
11. Harada, M.; Ohya, T.; Iida, K.; Hayashi, H.; Hirano, K.; Fukuda, H. *J. Appl. Polym. Sci.* **2007**, *106*, 1813.
12. Li, Y.; Shimizu, H. *Macromol. Biosci.* **2007**, *7*, 921.
13. Anderson, K. S.; Schreck, K. M.; Hillmyer, A. M. *Polym. Rev.* **2008**, *48*, 85.
14. Oyama, H. T. *Polymer* **2009**, *50*, 747.
15. Hashima, K.; Nishitsuji, S.; Inoue, T. *Polymer* **2010**, *51*, 3934.
16. Jiang, J.; Su, L.; Zhang, K.; Wu, G. *J. Appl. Polym. Sci.* **2013**, *128*, 3993.
17. Chen, G. X.; Kim, H. S.; Kim, E. S.; Yoon, J. S. *Polymer* **2005**, *46*, 11829.
18. Li, T.; Turng, L.-S.; Gong, S.; Erlacher, K. *Polym. Eng. Sci.* **2006**, *46*, 1419.

19. Yu, Z.; Yin, J.; Yan, S.; Xie, Y.; M, J.; Chen, X. *Polymer* **2007**, *48*, 6439.
20. Chow, W. S.; Lok, S. K. *J. Therm. Anal. Calorim.* **2009**, *95*, 627.
21. Balakrishnan, H.; Hassan, A.; Wahit, M. U.; Yussuf, A. A.; Abdul Razak, S. B. *Mater. Des.* **2010**, *31*, 3289.
22. Leu, Y. Y.; Mohd Ishak, Z. A.; Chow, W. S. *J. Appl. Polym. Sci.* **2012**, *124*, 1200.
23. Jiang, L.; Liu, B.; Zhang, J. *Ind. Eng. Chem.* **2009**, *48*, 7594.
24. Baouz, T.; Acik, E.; Rezgui, F.; Yilmazer, U. *J. Appl. Polym. Sci.* **2014**, 132.
25. Sinha Ray, S.; Maiti, P.; Okamoto, K.; Yamada, K.; Ueda, K. *Macromolecules* **2002**, *35*, 3104.
26. Pluta, M. *J. Polym. Sci.* **2006**, *44*, 3392.
27. Sinha Ray, S.; Okamoto, M. *Prog. Polym. Sci.* **2003**, *28*, 1539.
28. Baouz, T.; Rezgui, F.; Yilmazer, U. *J. Appl. Polym. Sci.* **2013**, *128*, 3193.
29. Mert, M.; Yilmazer, U. *J. Appl. Polym. Sci.* **2008**, *108*, 3890.
30. Acik, E.; Yilmazer, U.; Orbey, N. Rheological Properties of Poly (lactic acid) Based Nanocomposites: Effects of Different Organoclay Modifiers and Compatibilizers, submitted.
31. Gonçalves, C. M. B.; Coutinho, J. A. P.; Marrucho, I. M. In Poly(lactic acid): Synthesis, Structures, Properties, Processing, and Applications; Auras, R.; Lim, L.-T.; Selke, S.; Tsuji, H., Eds.; Wiley: Hoboken, **2010**; Chapter 8, p 97.
32. Dogan, K.; Gumus, S.; Aytac, A.; Ozkoc, G. *Fiber Polym.* **2013**, *14*, 1422.
33. Durgun, H.; Bayram, G. *J. Adhes. Sci. Technol.* **2012**, *19*, 407.
34. Chiu, H.-T.; Hsiao, Y.-K. *J. Polym. Res.* **2006**, *13*, 153.
35. Di, Y.; Iannace, S.; Di Maio, E.; Nicolais, L. *J. Polym. Sci., Part B: Polym. Phys.* **2005**, *43*, 689.
36. Kumar, M.; Mohanty, S.; Nayak, S. K.; Parvaiz, M. R. *Bioresour. Technol.* **2010**, *101*, 8406.
37. Kusmono Mohd Ishak, Z. A.; Chow, W. S.; Takeichi, T. *Rochmadi. Eur. Polym. J.* **2008**, *44*, 1023.
38. Peterson, L.; Oksman, K.; Mathew, A. P. *J. Appl. Polym. Sci.* **2006**, *102*, 1852.
39. Yeniova, C. E.; Yilmazer, U. *Polym. Comp.* **2010**, *31*, 1853.
40. Chang, J.-H.; An, Y. U.; Cho, D.; Giannelis, E. P. *Polymer* **2003**, *44*, 3715.
41. Baouz, T.; Fellahi, S. *J. Appl. Polym. Sci.* **2005**, *98*, 1748.